

Densitometric and finite-element analysis of bone remodeling further to implantation of an uncemented anatomical femoral stem*

A. Herrera^{a,b}, J.J. Panisello^{a,b}, E. Ibarz^c, J. Cegoñino^c, J.A. Puértolas^d and L. Gracia^c

^aDepartment of Surgery. University of Zaragoza. Zaragoza. Spain.

^bDepartment of Orthopedic and Trauma Surgery. Miguel Servet University Hospital. Zaragoza. Spain.

^cDepartment of Mechanical Engineering. University of Zaragoza. Spain.

^dDepartment of Materials Science and Technology. University of Zaragoza. Spain.

Introduction. Implantation of a femoral stem changes the load transmission dynamics in the hip and gives rise to the so-called adaptive remodeling. The goal pursued by all stems, whether cemented or not, is to achieve a perfect load transmission mechanism in order to avoid the phenomenon of stress-shielding, which may cause proximal bone devitalization.

Materials and methods. In order to quantify bone mass variations in the 7 Gruen zones, a serial DEXA analysis was carried out in 80 patients, with preoperative measurements as well as postoperative measurements at 6 months and 1, 3, 5, 7 and 10 years post implantation.

Results and conclusions. Finite-element (FE) simulations make it possible to characterize the biomechanical changes that occur in the femur further to implantation of a prosthetic stem, as well as the stem's long-term performance. The purpose of our study is to determine whether the results of the simulation can explain the biomechanical changes that may lie behind the evolution of bone density observed through DEXA scanning after implantation of an uncemented anatomical stem.

The results of the FE simulation show an excellent match between the bone loss observed on DEXA scans and the evolution of stress patterns observed in each of the Gruen zones, which confirms that even if the stem implanted was metaphyseal, stress shielding was manifest in the proximal femoral area, giving rise to the devitalization of bone in Gruen zones 1 and 7.

Key words: bone remodeling, DEXA scan, finite-element analysis, hip prosthesis.

Estudio densitométrico y con elementos finitos de la remodelación ósea tras la implantación de un vástago femoral anatómico no cementado*

Introducción. La implantación de un vástago femoral cambia las condiciones de transmisión de carga de la cadera, produciendo el denominado remodelamiento adaptativo. El objetivo de todos los vástagos (cementados y no cementados) ha sido conseguir una perfecta transmisión de cargas que evite los fenómenos de puenteo de fuerzas o *stress-shielding*, que a su vez producen una desvitalización ósea proximal.

Material y método. Para cuantificar las variaciones de la masa ósea en las 7 zonas de Gruen se ha realizado un estudio seriado a 10 años con DEXA en 80 pacientes, con mediciones en el pre y posoperatorio, 6 meses posoperatorio, y a 1, 3, 5, 7 y 10 años tras la implantación de la prótesis.

Resultados y conclusiones. La simulación con elementos finitos (EF) permite caracterizar los cambios biomecánicos que se producen en el fémur tras la implantación de un vástago protésico, así como su comportamiento a largo plazo. El objetivo de nuestro estudio es comprobar si los resultados de la simulación explican los cambios biomecánicos que justifiquen la evolución de la densidad ósea obtenida mediante el estudio con DEXA, tras la implantación de un vástago anatómico no cementado.

Los resultados de la simulación con EF presentan un perfecto paralelismo entre las pérdidas de masa ósea detectadas con la DEXA y la evolución tensional en cada zona de Gruen, lo que confirma que aunque el diseño de la prótesis es de apoyo metafisario, se produce un claro fenómeno de

Corresponding author:

A. Herrera.

Paseo de Isabel la Católica, 1-3.

50009 Zaragoza. Spain

E-mail: aherrera@salud.aragon.es

Received: August 2007

Accepted: October 2007

*SECOT Foundation Basic research award 2007.

punteo de fuerzas en la zona proximal del fémur, todo lo cual produce una desvitalización ósea en las zonas 1 y 7 de Gruen.

Palabras clave: remodelado óseo, estudio con DEXA, elementos finitos, prótesis de cadera.

Bone is a living tissue constantly undergoing change; this change consists in resorption and formation of new bone, without any variations in form, this process is known as remodeling. On the other hand, bone adapts its structure, following Wolff's Law, to the biomechanical forces and loads that impact it.

In the hip joint, the body load is transmitted to the femur head, from there it is transmitted to the medial cortical bone of the femur neck and from there it is transmitted to the lesser trochanter, from which it is distributed to the bone diaphysis.

Implantation of a femur stem, cemented or non-cemented, clearly alters, at bone level, the physiological transmission of loads, since these are now transmitted through the prosthetic stem, centripetally, from the central cavity of the cortical bone. This alteration of normal biomechanical processes of the hip causes the phenomenon known as adaptive remodeling¹, since the bone has to adapt to the new biomechanical process. During this remodeling, bone is affected by mechanical and biological factors. The mechanical factors are associated with the new load distribution mechanism related to the implant of a prosthesis in the femur and the physical characteristics of the implant (size, design, alloy), as also to the type of fixation of the femur implant²⁻⁶. The biological factors are related to the person's age and weight, initial bone mass, quality of primary fixation and load borne by the implant. The most important of all these factors is the initial bone mass².

The aim of all non-cemented prosthetic designs has been to achieve an optimum load transmission – of a physiological nature – from the metaphyseal zone to the rest of the femur, trying to avoid stress-shielding. Long term follow-up of different non-cemented stem models has shown that this is not possible to achieve⁷⁻¹⁴. It was also thought that if metaphyseal supported stems were coated with an osteoconductive substance such as hydroxiapatite (HA), which achieved good proximal osteointegration¹⁵, it would be possible to achieve better load transmission and prevent stress-shielding; the underlying rationale being that vertical forces transmitted by the stem would become horizontal forces that would be transmitted to the metaphyseal zone¹⁶.

The femur responds to stress-shielding in its proximal zone with bone devitalization that, once the bone loss is 30 to 40% of the bone mass, can be seen on a simple X-ray¹⁷; however, it is necessary to use densitometry with double energy X-rays (DEXA) to quantify and assess the evolution of this phenomenon over the years¹⁸⁻²⁰.

A 10 year study with DEXA of an anatomic stem with metaphyseal support and HA coating (ABG 1) has shown that there is devitalization of the proximal femur, which clearly indicates that there is stress-shielding, because the proximal part of the femur does not receive loads and, applying Wolff's Law, the decrease of stress in this zone causes loss of bone mass^{21,22}. This behavior does not correspond to that foreseen by the design.

Finite elements (FE) simulation makes it possible to establish the biomechanical changes that occur in the femur due to implantation of a prosthetic stem and the possible long-term consequences. There are many studies that have used different models to study the effects and interactions caused by a hip implant in the femur. Most of them focus on the mechanical behavior of different types of prosthetic implants under the effects of static and dynamic loads, or fatigue, and the influence of the material on this behavior²³⁻²⁶. The status of the loads applied in the finite model is especially important; there are studies²⁷ that analyze the application of different combinations of forces, although the most usual is to consider 2 loads: the reaction of the hip, seen in the femur head, and the reaction caused by action of the abductor muscles^{28,29}. There are, moreover, many studies of models of bone remodeling, but focused on short term results (1 to 2 months after surgery), or on the transition between the preoperative and the postoperative period³⁰⁻³².

The aim of this study is, first, to analyze the long-term changes of femur bone density after the implant of an anatomic, metaphyseal supported, HA coated, non-cemented femur stem (ABG-I). Second, to create 3D finite elements models of the healthy femur and the femur after the implant of an ABG-I stem, so as to study its mechanical behavior especially with reference to load stress transmission by contact between bones and prosthesis. And, finally, to establish whether the results of finite elements simulation makes it possible to explain the biomechanical changes that cause the evolution seen in the long term of this model of femur stem in the study with DEXA; and whether, therefore, this is a valid procedure to predict bone evolution in the long term.

We do not want to create models of bone remodeling, a subject widely reported in the literature³⁰⁻³³, only to verify the correlation between mechanical stimulation, measured in average stress values for each zone, and the changes seen in bone density.

MATERIALS AND METHODS

We designed a prospective controlled study to determine peri-prosthetic remodeling caused by an anatomically designed non-cemented ABG-I femur stem.

The size of the sample was calculated based on the average loss of bone density seen in previous studies for the 7

Gruen zones, which was, by cm^2 , 130 mg of $\text{HA}^{2,5,19,34-37}$, and the variation of bone density with relation to preoperative measurements. Therefore, it was considered necessary to include 60 patients, although finally we added 20 more with the aim of ensuring a minimum number of subjects during follow-up.

The inclusion criteria were:

- 1) First, a medical indication for this type of implant based on age, shape and quality of the femur.
- 2) Second, a diagnosis of primary arthritis of one unilateral hip joint, since the healthy hip was used as a control.
- 3) Finally, patients must accept inclusion in the study. The study had been approved for research purposes by the local Ethics Committee.

The patients included in the study were operated from February to October 1994. However, of the total 80 patients that complied with the inclusion criteria

Only 61 completed the 10 year follow-up (32 men and 29 women); at the moment of surgery, mean age was 59 years (range 38 to 76), and mean weight was 79.3 kg (range 49 to 110 kg).

All data of the 19 patients lost during follow-up were excluded from the study. These patients were lost to the study due to: 2 cases of neurological disease that did not allow the patients to walk normally, 3 cases of osteolysis that required revision of the stem, 8 cases of arthritis of the control hip that required replacement and 6 patients changed their domiciles and did not complete the follow-up.

The prosthesis used was an ABG-I femur stem (Stryker, Howmedica) and the acetabular cup used was of the same system, control of the evolution of which was not included in the study. This stem is anatomically designed, non-cemented and is implanted by press-fit at a metaphyseal level. The implant is proximally coated with 70 micron thick coat of HA, with a crystallinity of 97%, and a fish-scale design on the anterior and posterior facets to increase stability. The tail of the implant is thin and short to prevent contact with the diaphyseal endostium.

All patients were operated using a postero-lateral approach. The femur canal was prepared by diaphyseal burring (1 mm more than the diameter of the tail of the definitive implant) and progressive rasping until prosthesis fit was achieved, leaving 2-3 mm of cancellous bone surrounding the stem. The friction pair in all cases was a metallic head on a polyethylene cup.

Partial load-bearing using 2 crutches was allowed during the first 6 weeks and subsequently the crutches were set aside according to individual tolerance.

Clinical assessment during the preoperative period and the follow-up was carried out using the Merle-D'Aubigné score. Periodically, over 10 years, X-rays of each patient were taken, to determine the position of the implants or ob-

serve any other radiological findings that could indicate loosening according to Engh³⁸ criteria. The same observer assessed all the X-rays taken.

To assess evolution of bone mineral density we analyzed small 30 by 30 pixel areas centered in each of the 7 Gruen zones of the femur, both of the operated hip and the control hip, to ensure the exact location of each of the analyzed areas we used a special software to compare exams. All determinations were carried out with a HOLOGIC QDR 1000 (Hologic Inc, Waltham, Massachusetts) densitometer, using a metal exclusion program, of both hips during the preoperative period and at 10 years, with additional studies of the operated hip at 15 days, 6 months, and 1, 3, 5 and 7 years postoperatively. However, considering that the remaining bone after prosthesis implant would undergo remodeling, we used bone density values taken postoperatively as a reference for subsequent comparisons. We considered that appropriate patient positioning was of maximum importance to ensure the feasibility of exams, so we developed a protocol for patient positioning^{39,40}. Patients were positioned on the scanner table, on their backs, supine, with hips and knees extended and with the limb in a neutral position attached to a rigid plastic device by means of Velcro tapes. The technical characteristics of the densitometer used were: femur precision error 1.5 to 2%; exactitude error 2 to 4%, up to 10% in obese patients, patient radiation less than 3 mRem and length of time of exam 8 minutes.

For the statistical analysis of the data obtained during follow-up, we first carried out an ANOVA test with a level of significance of 0.05 for bone density data in each femur zone. When differences were found we carried out a Student "t" test with a level of significance of 0.025 to compare the results of preoperative density with those obtained during each moment of the follow-up. Finally, we carried out another Student "t" test for paired data, with the aim of comparing the density of the operated hip and the healthy hip at 10 years.

For FE simulation we used a cadaver femur, taken from a 60 year old healthy person, who died in a traffic accident, and a hip prosthesis, type ABG-I with a HA coated stem (right side, size number 3, the most frequently used in clinical practice, code RFE4841-103).

For the non implanted femur model we used a Roland PIZCA 3D Laser scanner. We scanned the femur using the Dr. Pizca 3 and 3D editor programs. By femur scanning we obtained a geometric model that did not distinguish amongst the materials of its components: cortical bone, cancellous bone and bone marrow. To establish the geometry of cancellous bone we used computerized axial tomography (CAT) scans (General Electric Brightspeed Eltie) 30 transverse tomographic sections and 8 longitudinal ones. Horizontal sections were every 5 mm. Subsequently, we established an initial mesh of the surfaces of the different scanned areas and using *I-deas*⁴¹ we obtained a 3D mesh

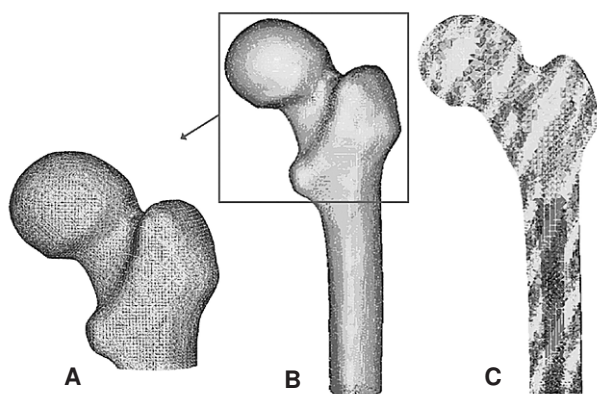


Figure 1. (A) Details of the mesh in the proximal area of the healthy femur model; (B) finite elements model of a healthy femur; (C) longitudinal section of a healthy femur model.

(Figure 1) with introduction of contour conditions. The model was based on tetraedric type elements with linear approximation.

To develop the prosthesis model we carried out hip arthroplasty surgery on the cadaver femur, implanting a prosthesis in the same way as we would in a clinical case. This operated femur was scanned a second time to use it as a guide for the positioning of the prosthesis.

Once we had scanned the ABG-I prosthesis and imported the three meshes from *I-deas* (healthy femur, ABG-I prosthesis and operated femur), we eliminated, on the computer, the epiphysis of the cadaver femur, with sections similar to those used in surgery, to be able to insert the prosthesis, and we subsequently positioned the prosthesis in the femur, always using as a guide the third mesh (Figure 2). From the former process of cadaver femur modeling we only used the cortical bone and modeled the cancellous bone again based on this, so that it was perfectly adjusted to con-

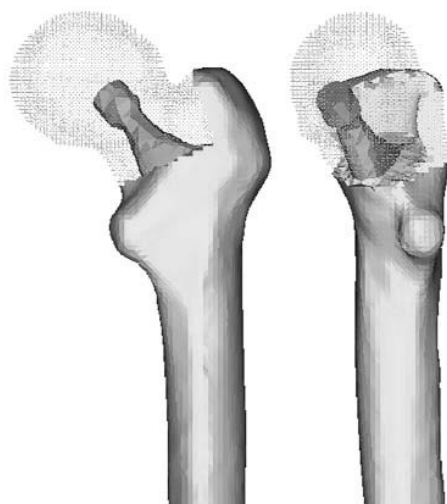


Figure 2. Both models superimposed.

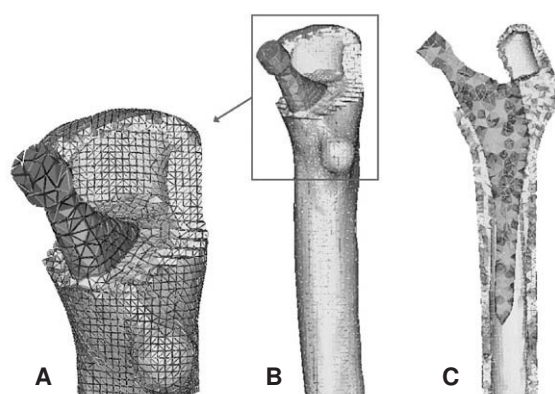


Figure 3. (A) Detail of the mesh in the proximal area of an ABG prosthesis; (B) finite elements model of a femur with an ABG-I prosthesis; (C) longitudinal section of a femur with an ABG-I prosthesis.

tact with the prosthesis (Figure 3). We used the Abaqus 6.5⁴² program to calculate and simulate previously generated models, and for subsequent visualization of results we used the *Abaqus Viewer* program.

The first model of a healthy femur had 408,518 elements (230,355 were of the cortical bone, 166,220 of the cancellous bone and 11,943 of the bone marrow), although later this number of elements was reduced, since the same precision was obtained with less calculations. Therefore, the final ABG-I prosthesis model had 60,401 elements (33,504 were of the cortical bone, 22,088 of the cancellous bone and 4,809 of the ABG-I prosthesis).

The ABG-I prosthesis is made of a wrought titanium alloy type Ti-6Al-4V. This material is certified by ASTM/ISO Standards with the code F136/5832-3. Table 1 shows a summary of the diverse mechanical properties used in the prosthesis, as also the biological materials considered isotropic. These values have been taken from the specialized literature on the subject⁴³⁻⁴⁵. The prosthesis is three times more rigid than cancellous bone. This huge difference makes it possible, in the case of the model with the prosthesis, to suppose the prosthesis is a rigid solid, since, as both are in contact, all the deformation will be absorbed by cancellous bone, and the prosthesis will remain intact during deformation. The joint between prosthesis and bone is not modeled or mathematically defined; however, conditions of contact with friction are defined (applying the friction coefficient 0.5).

There are many previous studies that include a comparative analysis for different combinations of muscle loads, which conclude that it is most appropriate to consider the loads of the *gluteus medius*, the *iliotibial* and the *iliopsoas*, or only the action of abductor muscles. In this study, we have used this last option because it is the one most used by the majority of authors. In general, the muscle force generated in the abductors is double that of body weight, and this causes a reaction on the femur head of 2.75 times this

Table 1. Mechanical properties used

Materials	Elastic Module (MPa)	Poisson Coefficient	Stress Maximum Compression (Mpa)	Stress Maximum Traction (Mpa)
Cortical bone	20.000	0,3	150	90
Cancellous bone	959	0,12	23	
Bone marrow	1	0,3		
ABG-I Prosthesis	114.000	0,33		

weight. However, in the instant the heel hits the ground and during double contact this load increases up to 4 times the value of body weight⁴⁶. to be able to impose contour conditions, we have considered this last case, because it is the most unfavorable, and the average weight seen in densitometry studies was used: 79.3 kg of body weight. Three contour conditions arise, complete block of the medial part of the femur, force applied on the head of the femur due to the reaction of the hip due to the person's weight, and force on the major trochanter generated by the abductor muscles. The direction of the forces can be seen in Figure 4 in the cadaver femur and in Figure 5 for the ABG-I prosthesis. A decision was made to fixate the medial area rather than the distal area, as we consider it is sufficiently far from the proximal bone, and therefore allows us to reduce the cost of calculations by not using the whole femur. This model is

comparable to those that have contour conditions consistent with distal fixation, since the loads applied practically coincide with the direction of the femur axis and this reduces the differences in comparison with the final values.

To be able to carry out an analysis with finite elements the cortical bone of each of the models is divided into 7 zones that coincide with the so called "Gruen zones". As has been mentioned, all materials are considered isotropic with linear elasticity. Using as a reference several published studies^{32,33,47} we established a relation between values of bone mass provided by the medical study²² and apparent density, and between this and the elastic pattern, we obtained the values for the pattern of cortical bone elasticity for each of the 7 Gruen zones. These values are successively adjusted for each of the models at different moments in time: during the postoperative period: (15 days after surgery), 6 months, 1, 3, 5, 7 and 10 years for the ABG-I prosthesis, and 10 years in the case of the healthy femur. Both models have initial data (collected during the preoperative period). In this way, we were able to adjust the mechanical properties of bone over time, as would happen in reality.

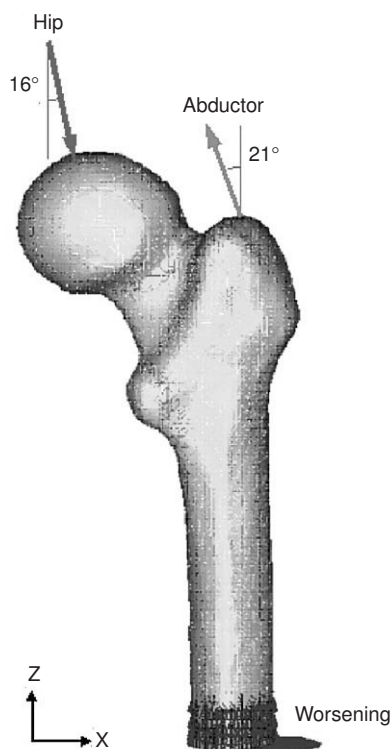


Figure 4. Finite-element model with contour conditions of a healthy femur.

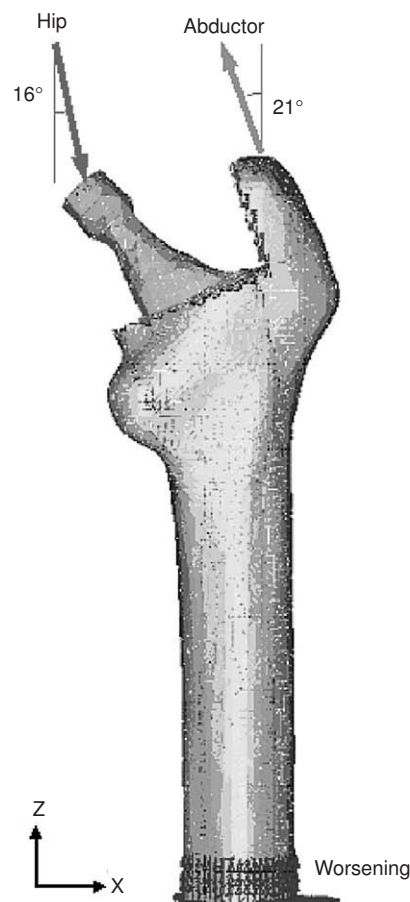


Figure 5. Finite-element model with contour conditions of a femur with an ABG-I prosthesis.

Table 2. Changes in operated hip bone density during follow-up after surgery

	Pre-op (reference)	Post-op	6 months	1 year	3 years	5 years	7 years	10 years
Femur 1:	746	680	622	596	591	609	607	594
DE	169,5	145,4	228,5	182,3	144,9	153,4	213,1	188,1
Mín-máx	385-1.167	389-986	322-1.268	349-1.195	337-987	349-1.078	361-1.168	376-776
IC 95%			-174,3; -1,3	-159,6; -75,2	-167,6; 79,0	-175,3; -78,8	-225,1; -15,1	-290,4; -50,3
% Change		-8,84%	-8,52%	-12,35%	-13,08%	-10,44%	-10,73%	-12,64%
p			0,047	0,002	0,004	0,008	0,032	0,020
Femur 2:	1.166	1.125	1.072	1.095	1.062	1.083	1.187	1.138
DE	265,2	209,0	291,5	276,7	233,3	240,3	409,0	344,8
Mín-máx	773-1.772	607-1.655	680-1.769	667-1.948	677-1.709	688-1.757	556-1.719	568-1.669
IC 95%			-153,8; 15,5	-125,2; 32,7	-139,9; 35,7	-147,5; 40,8	-302,0; 223,7	-291,4; 243,2
% Change		-3,51%	-4,71%	-2,66%	-5,66%	-3,73%	+5,51%	+1,01%
p			0,104	0,239	0,240	0,355	0,718	0,668
Femur 3:	1.488	1.411	1.299	1.374	1.324	1.329	1.418	1.354
DE	282,4	181,6	263,8	260,3	217,7	233,2	305,5	293,5
Mín-máx	968-2.079	1.072-1.809	941-1.913	853-2.103	865-1.810	853-1.819	972-1.897	877-1.835
IC 95%			-194,2; -38,4	-141,5; 5,5	-136,2; 21,0	-136,4; 33,3	-307,2; 80,4	-461,5; 274,6
% Change		-5,17%	-7,93%	-2,62%	-6,16%	-5,81%	+0,49%	-4,03%
p			0,006	0,069	0,143	0,285	0,193	0,478
Femur 4	1.582	1.482	1.485	1.497	1.459	1.461	1.467	1.433
DE	273,5	211,9	263,4	231,4	228,3	240,4	289,7	315,1
Mín-máx	1.119-2.122	1.039-1.916	1.025-2.076	1.094-2.008	1.090-2.174	1.087-2.008	1.085-2.036	1.065-2.016
IC 95%			-46,2; 68,9	-54,3; 71,8	-60,1; 77,4	-72,7; 66,8	-333,0; 251,3	-371,5; 227,6
% Change		-6,32%	+0,20%	+1,01%	-1,55%	-1,41%	-1,02%	-3,30%
p			0,634	0,776	0,769	0,980	0,734	0,907
Femur 5	1.545	1.462	1.440	1.446	1.425	1.426	1.482	1.442
DE	360,0	301,6	284,3	273,5	285,7	299,9	356,9	321,5
Mín-máx	934-2.589	870-2.250	868-2.106	805-2.174	801-2.176	815-2.164	910-2.140	906-2.142
IC 95%			-149,7; -3,2	-150,1; 7,5	-158,1; 10,3	-180,1; -2,5	-345,6; 285,9	-344,5; 299,7
% Change		-5,37%	-1,50%	-1,09%	-2,53%	-2,46%	+1,36%	-1,37%
p			0,401	0,274	0,083	0,094	0,459	0,288
Femur 6	1.353	1.317	1.188	1.197	1.258	1.261	1.331	1.327
DE	383,7	315,1	309,4	310,8	309,8	320,8	474,2	350,9
Mín-máx	695-2.386	750-2.045	594-1.968	657-1.927	645-1.997	664-1.935	646-2.201	643-2.209
IC 95%			-331,7; -84,2	-316,8; -62,9	-334,7; -73,7	-377,2; 86,9	-564,4; -528,1	-445,3; -302,8
% Change		-2,66%	-9,79%	-9,11%	-4,47%	-4,25%	+1,06%	+0,7%
p			0,002	0,005	0,064	0,070	0,935	0,456
Femur 7	1.285	1.172	896	852	803	791	733	669
DE	304,2	305,6	321,9	310,3	299,7	317,0	282,1	274,6
Mín-máx	634-1.997	643-2.056	474-1.671	409-1.848	390-1.788	392-1.648	375-1.180	398-1.025
IC 95%			-423,1; -247,8	-436,9; -252,1	-427,0; 260	-440,3; -280,	-659,2; -235,	-719,1; -139
% Change		-8,79%	-24,06%	-27,3%	-31,4%	-32,5%	-37,45%	-42,91%
p			0,001	0,001	0,001	0,001	0,003	0,018

Bone density is expressed in milligrams of HA per cm². The variation percentage is related to the preoperative scan, considered as the value of reference. SD: Standard deviation; CI: confidence interval.

RESULTS

The 61 patients that completed the densitometry study had good clinical evolution (their mean score using the Merle D'Aubigne scale was 16.90 points), with absence of significant complications during follow-up. Radiologically all the stems were considered stable, with absence of significant cortical hypertrophy; however, condensation of cancellous bone was seen in zones 2, 3, 5 and 6 in more than 80% of the patients, and bone resorption in zone 1 in 32% of them and in zone 7 in 68%.

The evolution of bone density in the operated and healthy femurs is shown in tables 2 and 3 respectively. Pre-

operative measurements carried out on both hips, showed slightly higher numbers in healthy femurs, from 0.1% in zone 6 to 4.3% in zone 2, although these differences were not statistically significant and can be attributed to discreet secondary bone atrophy secondary to less loading of the extremity due to pain and loss of hip mobility.

The figures seen during the postoperative period were taken as a reference for operated femurs. Differences of 2.66 to 10.01% were detected in comparison with measurements prior to surgery, and these changes were attributed to the bone loss caused by burring and rasping during prosthesis implant. Six months after surgery a decrease in bone

density was seen in all areas except zone 4, which was attributed to relative rest, partial load-bearing and the late effect on the bone of preparation for surgery.

The changes in bone density in the second semester reflect the response of bone to the new biomechanical situation caused by prosthesis implant. An additional discreet loss of bone was seen in zones 1 and 7, as also a slight recovery in the middle and distal zones surrounding the implant. These changes suggest that there is an effective stress transmission from the stem to zones 2 and 6, capable of promoting preservation and even a certain degree of recovery of bone density in those areas and other more distal ones. In the same way, the loads transmitted to zones 1 and 7 seem not to be sufficient to stimulate bone preservation of these zones.

No significant changes in bone density were seen in zones 1 to 6 from the end of the first year up to the end of the tenth year. The bone mass remained stable during that period, with minimal repercussions in zones 2 and 6. However, a decrease was seen in zone 7 during the period between the fifth and tenth years, at which time a loss of 42.9% was seen. To determine the causes of this late loss the corresponding X-rays were reviewed and it was seen that all the stems showed signs of radiological stability, but that there was bone resorption, visible on simple X-rays, in two thirds of cases.

The bone density of the contralateral healthy hip showed slight differences during follow-up, with variable decreases from 0.9 to 7.2%, more evident in the proximal part of the femur, rich in cancellous bone. The values obtained for zones 2 to 6 were similar to those seen in operated femurs, only zones 1 and 7 showed significant differences, as occurs with variations in stress (figures 6 and 7). Measurements of von Mises stress have been used because this is a relevant variable and of standard use in finite element software.

The results obtained in each of the models based on the finite elements simulation are compared, and an attempt is made to correlate these values with clinical studies in patients²². In the case of the healthy hip, we have data for two moments in time, an initial moment, at the beginning of the study, and a second moment after 10 years. In Figure 8 (A and B) it is possible to observe von Mises stress distribution in the model at these 2 moments in time. The same scale was used in all cases to make the comparison easier. It can be seen how the medial side of the femur is the most affected due to the eccentricity of the loading.

The implanted hip model was studied clinically at 8 different moments in time: initially during the preoperative period, and then during the postoperative period (15 days after implant), at 6 months and after 1, 3, 5, 7 and 10 years. In Figure 9 (A and B) it is possible to see the evolution of von Mises stress at different moments in time. In

cancellous bone (Figure 9B), in the zone where the prosthesis HA comes to an end, it is possible to see an increase over time of the intensity of the load, which indicates its transmission by a funnel effect instead of friction. With the same initial bone mass values, cortical bone of the proximal zone of both models is studied. By analyzing the Mises stress distribution in Gruen zones 1, 2, 6 and 7 during the preoperative period and at 10 years (Figure 10), it is possible to see a decrease in stress on the operated femur in comparison with the healthy one, the result of proximal off-loading.

Table 3. Changes in bone density of the contralateral healthy hip during follow-up

	Pre-op	10 years
Femur 1:	782	737
DE	296,2	276,8
Mín-máx	401-1265	378-1.131
IC 95%		-131,4; 40,5
% Change		-5,8%
p		0,258
Femur 2:	1.093	1.026
DE	277,3	289,7
Mín-máx	698-1.527	681-1.525
IC 95%		-119,5; 42,8
% Change		-6,2%
p		0,345
Femur 3:	1.429	1.374
DE	288,9	261,4
Mín-máx	991-1.978	852-1.817
IC 95%		-159,8; 16,2
% Change		-3,9%
p		0,756
Femur 4:	1.591	1.599
DE	277,9	272,5
Mín-máx	1.177-2.006	1.096-2.095
IC 95%		-65,9; 109,1
% Change		0,5%
p		0,665
Femur 5:	1.530	1.516
DE	349,7	315,5
Mín-máx	907-2.421	896-2.258
IC 95%		-155,6; 11,7
% Change		-0,9%
p		0,461
Femur 6:	1.302	1.254
DE	309,8	291,8
Mín-máx	623-2.187	595-1.992
IC 95%		-277,9; 55,9
% Change		-3,7%
p		0,070
Femur 7:	1.192	1.106
DE	285,7	292,0
Mín-máx	611-1.819	499-1747
IC 95%		-291,4; -44,1
% Change		-7,2%
p		0,064

Bone density is expressed in milligrams of HA per cm². SD: Standard deviation; CI: confidence interval.

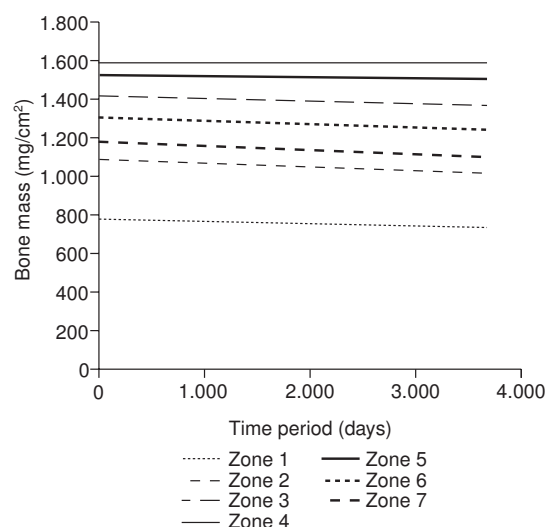


Figure 6. Bone mass over time in the healthy femur.

DISCUSSION

Adaptive remodeling after total replacement of the hip has multiple causes^{2,9,12}. to precisely quantify the changes in bone density that occur in the femur due to this process it is necessary to use a series of long term DEXA studies⁴⁸. Simulation using FE makes it possible to explain biomechanical changes that take place in the femur after prosthesis implant. This is a pioneer study that has the aim of determining if it is possible to correlate findings using DEXA with simulation models using finite elements in the analysis of long term evolution of bone density.

DEXA studies performed 3 and 6 months after surgery show decreases in bone mass that can vary from 20 to 50%, according to the prosthesis used and study methods. These losses are caused by several factors, rest and decreased ac-

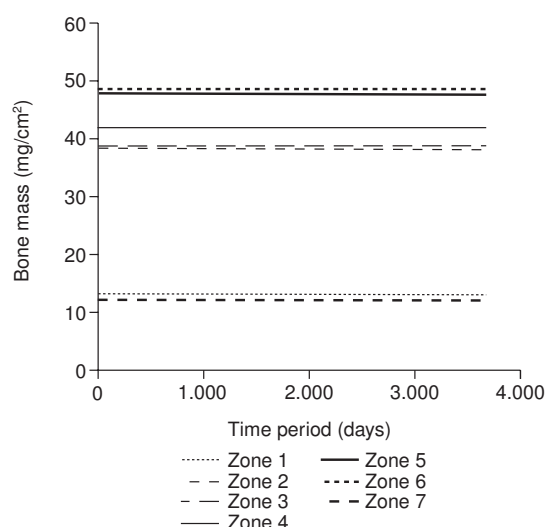


Figure 7. Average von Mises stress over time in a healthy femur.

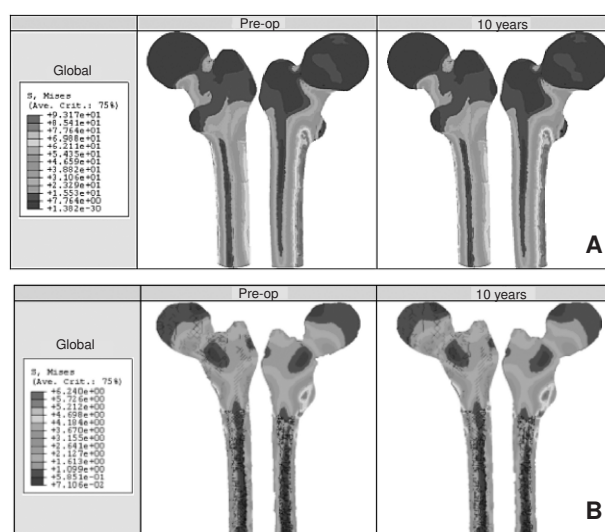


Figure 8. (A) von Mises stress in a healthy femur; (B) view of von Mises stress values in a longitudinal section of cancellous bone.

tivity are considered the most important, to which we must add the effects of surgery. We must first consider the preparation of the femur with burs and rasps that causes an immediate decrease of bone stock^{18,35}, which, in our study, varied from 2 to 10%, and that is not attributable to remodeling; so that postoperative measurements were taken as a reference to compare the evolution of bone density. However, the effects of the surgical technique used go beyond the immediate postoperative period. Femur rasping and the

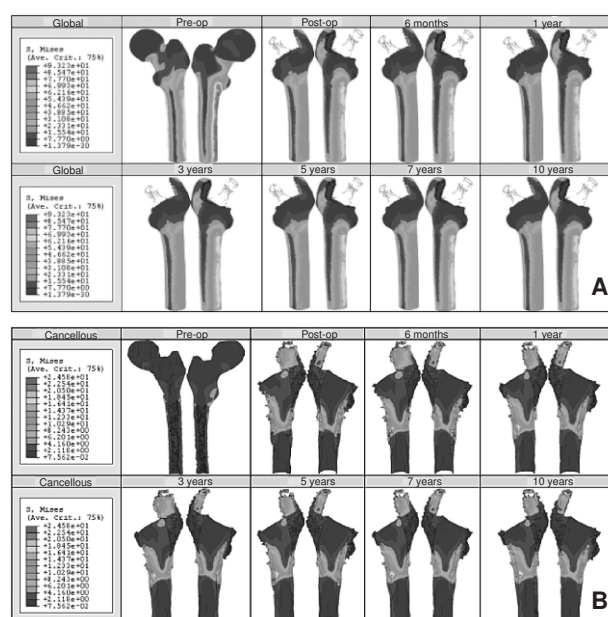


Figure 9. (A) von Mises stress in an ABG-I prosthesis; (B) detail of von Mises stress in a longitudinal section of cancellous bone.

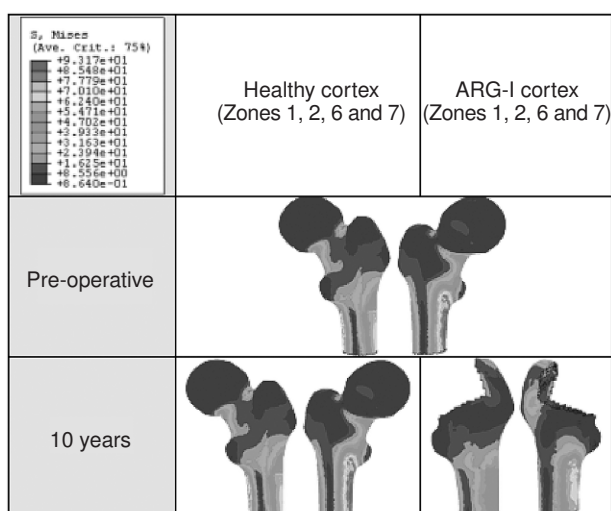


Figure 10. von Mises stress in cortical bone (Zones 1, 2, 6 and 7) of a healthy femur and a femur with an ABG-I prosthesis.

press-fit implant of the stem cause additional microfractures in the cancellous bone surrounding the implant, and this bone tissue will subsequently undergo necrosis and resorption, causing additional decreases of bone density that will be detected at the end of the sixth month. But the magnitude of these changes is not homogeneous, in middle and distal zones the damage to endosteal circulation caused by rasping and burring may cause partial necrosis of the internal part of the cortical bone, and this will take weeks to recover^{49,50}. to this must be added the devascularization and denervation caused by femur neck exposure for osteotomy. And added to these effects is the fact that this zone does not receive an appropriate load transmission, all of which explains the decrease in bone density of up to 32% at the end of the first year.

In the case of finite elements simulation, as can be seen in Figure 11, and always taking as a reference postoperative measurements, it is possible to see that in the middle and distal zones, up to 6 months post surgery, stress remains practically constant or increases slightly, which is favorable to the subsequent increase in bone density in these zones. However, during the same period of time, in the proximal femur zone, stress decreases by 3 to 11%, that is, as suspected, there is stress-shielding that causes loss of bone mass, as can be seen in Figure 12. It is not possible to compare these results with previous simulations as, up to now, such long term studies have not been performed.

In general, it is accepted that most adaptive remodeling has become established at the end of the first year, with a balance achieved in bone density of all zones from that moment on^{2,5,51-53}. The results seen in this study suggest that this stability is achieved between the sixth and the twelfth month, when, following Wolf's Law, the changes in bone density reflect the biomechanical response of bone. After

this period, bone density shows no significant changes during a period of 10 years. Only in zone 7 is it possible to see additional late decreases which we consider can be attributed to proximal atrophy due to stress-shielding. This decrease of bone density in a zone with reduced load transmission does not seem to have mechanical or biological consequences in other bone areas, however, a greater proximal atrophy may affect the stability of the implant and make the femur more vulnerable to fractures. In one third of all patients, late bone mass losses are seen, attributable to osteolytic cystic lesions in the neck of the femur, but without clinical repercussions at the time of follow-up.

In finite elements simulation, according to what can be seen in figure 11, stress variation ends around the end of the first year, and practically constant levels of stress are maintained in all zones. Therefore, there are no significant changes in bone density. The exception is zone 7, in which there is an additional unloading in the long term, and its bone density, therefore, continues to decrease. In Figures 13 to 18 it is possible to see in detail the evolution of bone mass density and stress levels in each zone over time. To do this we have represented the increase/decrease of bone mass and stress (percentages) taking as initial values postoperative measurements, which we consider the starting point of adaptive remodeling. Therefore, it is possible to see, in zones 2 to 6, middle and distal zones, that stress variations are much less than in proximal zones, with losses of stress of around 1-2%, in comparison with values of 3 to 5% in zone 1, and losses of 11 to 23% seen in zone 7.

When this anatomic metaphyseally-supported prosthesis was designed it was thought that its implant by press-fit in the metaphyseal zone could be capable of converting the loads received by the femur head in compression forces at a metaphyseal level, which could then be transmitted to distal

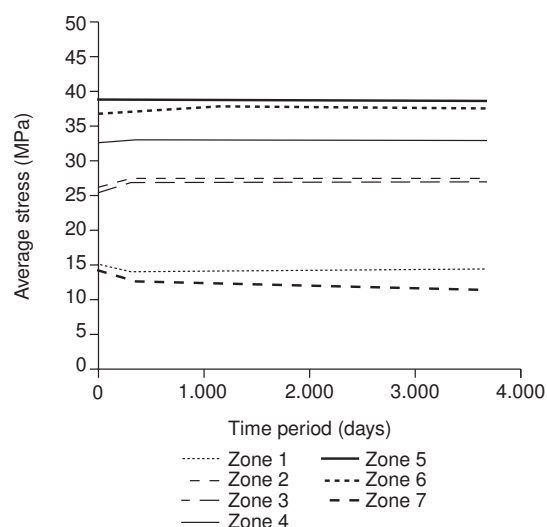


Figure 11. Average von Mises stress over time of a femur with an ABG-I prosthesis.

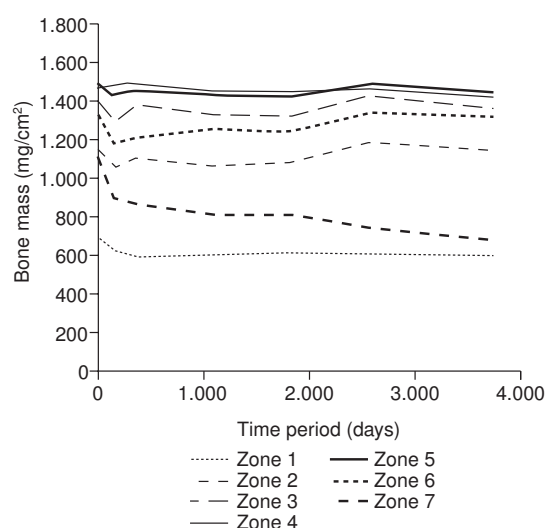


Figure 12. Bone mass over a period of time in a femur with an ABG-I prosthesis.

zones, preventing stress-shielding. At the end of the first year it is possible to see changes in bone density attributable to proximal atrophy due to stress-shielding, both in the DEXA study and by FE simulation. In the healthy femur the loads are transmitted from the femur head to the lesser trochanter, which distributes compression forces to the femur diaphysis³⁴. After prosthesis implant, this load model is inverted, and a funnel effect is caused, as is shown in the FE simulation (Figure 9B). Most compression forces are distributed from the stem to the diaphyseal zones, leaving the proximal femur free of load, and causing bone resorption. In Figure 19 it is possible to see the flow of stress generated at the femur head in a healthy femur, in comparison with an implanted femur. These figures have been obtained by means of a diagram of the stress flow in each model using Abaqus software. In this way it is possible to identify, in the healthy femur, the main trabecular bundles, i.e. the arcuate bundle of Gallois and Bosquette where the trabeculae exert traction forces, and the compressive supporting bundle of Delbet³⁶. In contrast to what happens in the healthy femur, in the femur with a prosthetic implant, it is seen that the main stresses are transmitted from the head of the prosthesis to the stem, therefore causing proximal unloading, and the femur receives the transmission of forces mainly in the zones at the end of the HA coating, causing the funnel effect. These changes in hip biomechanics explain why using non-cemented first generation stems causes bone density losses in proximal zones of up to 45%^{2,4,54}; that with second generation prosthesis they are still of up to 20 to 25% at the end of the first or second year, and that with wedge-shaped stems these values decrease to 10 to 30%^{5,20}. With made to measure stems, bone density losses in proximal zones are reduced to 10 to 15% at the end of the first year^{53,57}; with femur stems of reduced rigidity decreases in bone density of

up to 15% have been seen in the femur neck at the end of the second year^{6,55,58}.

During the theoretical design we also considered that the addition of HA coating at a metaphyseal level would optimize prosthesis integration at this level, as has been seen in autopsies of operated patients¹⁵. However, according to the results of this study, it has been proven that the improvement in osteointegration only contributes to stem stability, but does not influence bone remodeling. The remodeling pattern seen with this anatomic, non-cemented stem is similar to that seen with cemented second generation stems, in which, it was possible to see, using densitometry studies, decreases of bone density of up to 20 to 25 % in proximal zones, of 5 to 15% in intermediate zones and no appreciable changes in distal zones^{5,55,56,59}. These studies have also described how these changes remained stable after the first or second year after surgery.

In the long term remodeling may be affected by changes in bone density related to age, by secondary osteolysis due to polyethylene wear particles and by proximal bone atrophy due to stress-shielding.

Several studies show that aging affects both cortical and endosteal bone^{2,8,54,60}. However, in the patients included in this study, the bone loss detected in the healthy hip (from 0.9 to 7.2%) was located mainly in cancellous bone, and only minimal variation was detected in cortical bone. This data coincides with the differences in femur bone density seen for the population of our country in the groups of 50 to 59 years of age and 60 to 69 years of age⁶¹. These differences, furthermore, were significant only in proximal areas, and are attributable to prosthesis implant. All these findings suggest that in patients that are 60 years of age at the moment of surgery, little change in bone density can be expected over the next 10 years, as long as they maintain normal physical activity. The implant studied seems to provide a load transmission model capable of preserving a similar bone density in middle and distal zones as that seen in the healthy femur.

The data described for bone density agree with the results of the simulation study, in which a marked irregularity is seen in the long term, with increasing and decreasing stress variations, with quite irregular behavior (Figures. 15-18), comparable to what happens with bone density. The lowest levels of stress are seen in proximal zones, followed by zones 2 and 3, due to proximal unloading and the fact that they are located on the outer side, and the highest levels are seen in zones 5 and 6, due to both factors, the funnel effect and the fact that they are on the medial side of the femur (Figure 11). Finally, the correlation between the evolution of bone density and the evolution of stresses is almost perfect in zones 1 and 7, so that if a ratio is established between increases in bone density (%) and increases in stress (%), practically horizontal lines are obtained (Figure 20).

In conclusion, we wish to point out that the initial aim of designing and implanting a metaphyseal supported stem

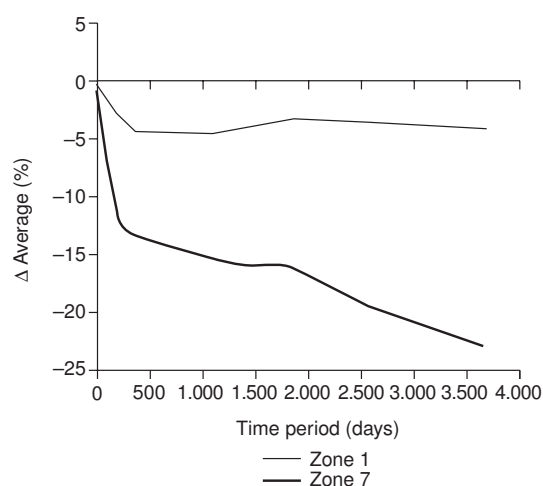


Figure 13. Variation of average von Mises stress (%) over time in Gruen zones 1 and 7 in a femur with an ABG-I prosthesis.

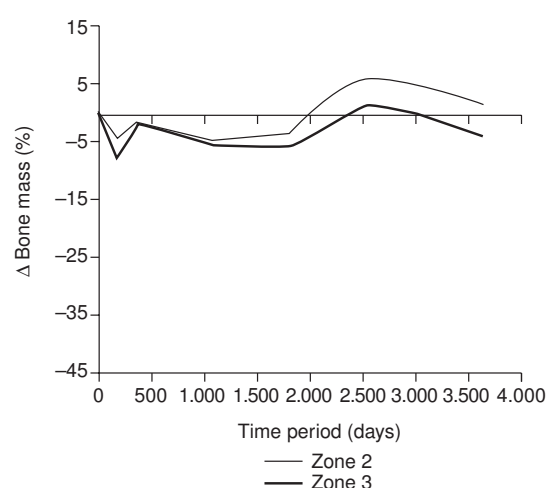


Figure 16. Variation of Bone mass (%) over time in Gruen zones 2 and 3 in a femur with ABG-I prosthesis.

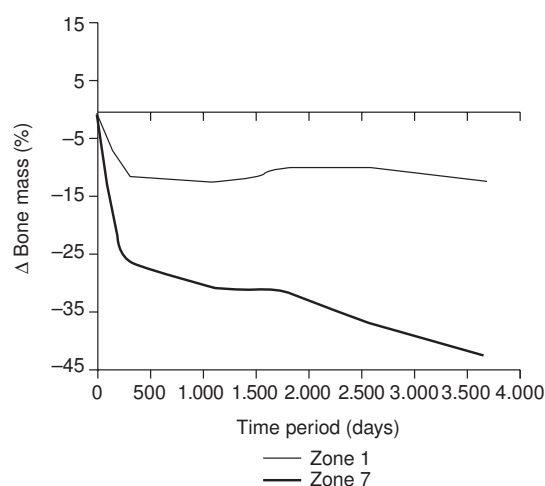


Figure 14. Variation of bone mass (%) over time in Gruen zones 1 and 7 in a femur with an ABG-I prosthesis.

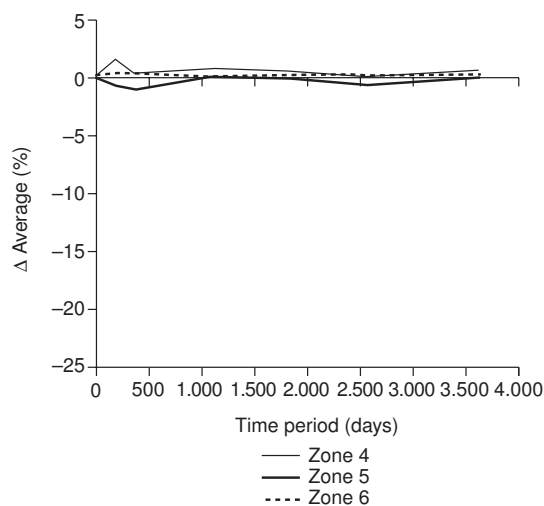


Figure 17. Variation of average von Mises stress (%) over time in Gruen zones 4, 5 and 6 in a femur with ABG-I prosthesis.

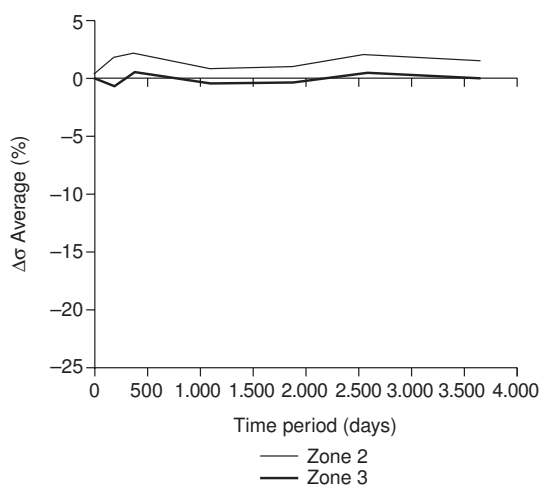


Figure 15. Variation of average von Mises stress (%) over time in Gruen Zones 2 and 3 in a femur with an ABG-I prosthesis.

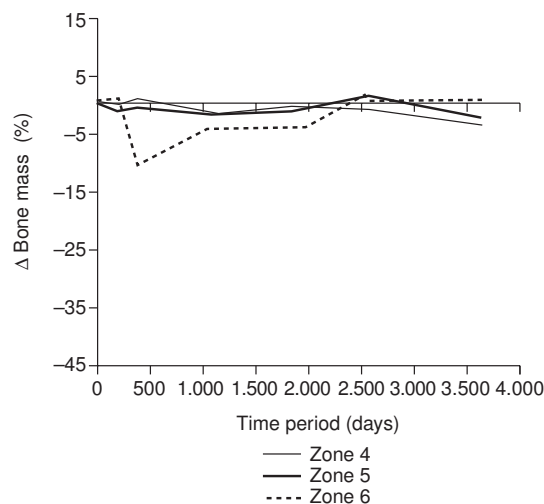


Figure 18. Variation of Bone mass (%) over time in Gruen zones 4, 5 and 6 in a femur with ABG-I prosthesis.

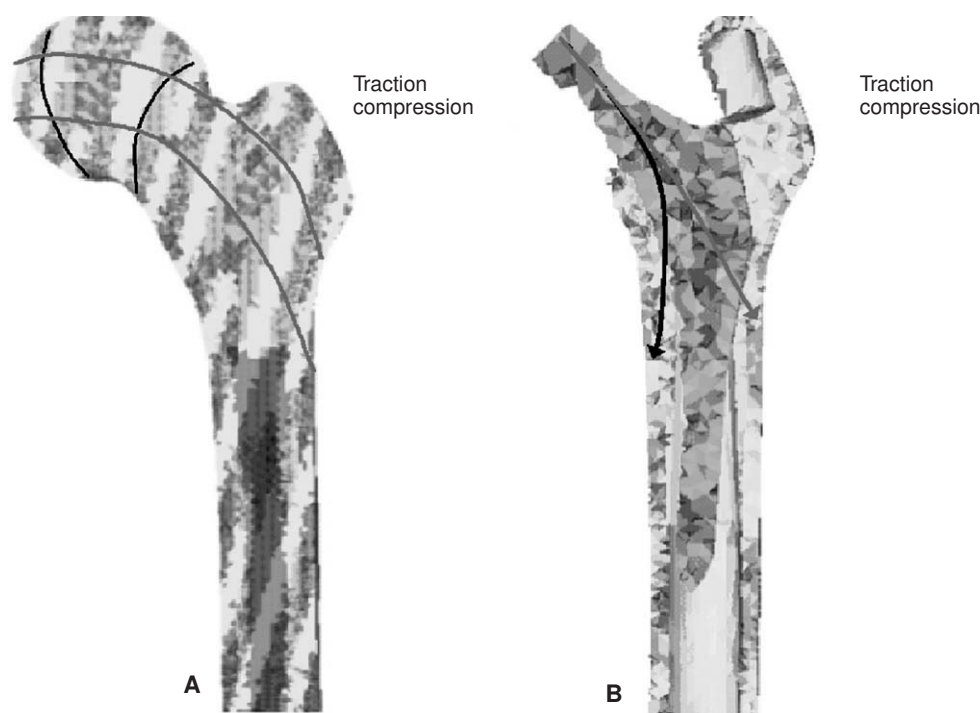


Figure 19. Stress flow-lines in a healthy model (A) and in a model with an ABG-I prosthesis (B).

was to achieve a transmission of forces in the femur, from proximal to distal, capable of preventing stress-shielding. This was not achieved, the remodeling seen with the ABG-I stem is similar to that seen with other anatomical designs.

The remodeling pattern caused by the ABG-I stem becomes established during the period between the sixth and twelfth month, and remains stable during the next 10 years after prosthesis implant. In relatively young patients the changes in bone density attributable to age are only slightly relevant during the 10 years subsequent to surgery, and do not affect

the stability of the implant. However, it is necessary to determine their effect over longer periods of time. The remodeling changes seen in the femur remain stable unless the metabolic, biological or mechanical conditions of the femur change.

Finite elements simulation are able to explain the biomechanical changes seen in the femur after stem implant, and allowed us to establish an evident parallel between the results obtained with DEXA studies and the results obtained with this simulation as can be seen in Figures 13 to 18, which show a perfect correlation between the changes in bone mass and the evolution of stress obtained by simulation in each of the Gruen zones. The good correlation seen between the results of the simulation and the densitometric studies allowed us, on one hand, to explain from the biomechanical point of view the changes seen in bone density in the long term, since it is clear that these are due to different ways of load transmission in the implanted femur in comparison with the healthy femur; and on the other hand, it allowed us to confirm the validity of simulation model; it can, therefore, be used under different conditions and for different time periods to predict with a certain precision the evolution of bone density based on the biomechanical behavior of femur-prosthesis interaction.

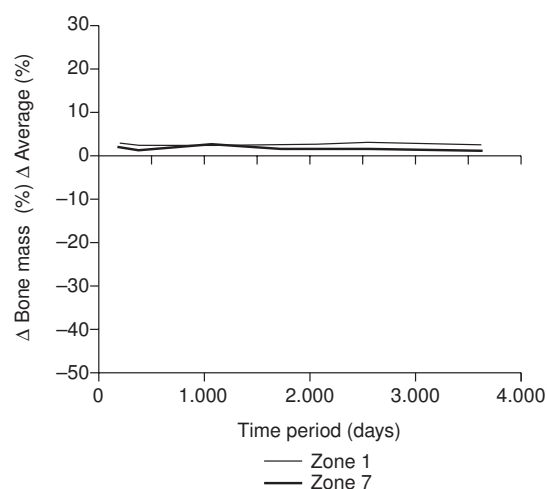


Figure 20. Correlation between increase in bone mass and average von Mises stress over time in Gruen zones 1 and 7 in a femur with an ABG-I prosthesis.

REFERENCES

1. Huiskes R, Weinans H, Dalstra M. Adaptive bone remodeling and biomechanical design considerations for noncemented total hip arthroplasty. *Orthopedics*. 1989;12:1255-67.

2. Sychter CJ, Engh CA. The influence of clinical factor on periprosthetic bone remodelling. *Clin Orthop*. 1996;322:285-92.
3. Rubash HE, Sinha RK, Shanbhag AS, Kim SY. Pathogenesis of bone loss after total hip arthroplasty. *Orthop Clin North Am*. 1998;29:173-86.
4. McAuley J, Sychterz CH, Engh CA. Influence of porous coating level on proximal femoral remodelling. *Clin Orthop*. 2000;371:146-53.
5. Gibbons CER, Davies AJ, Amis AA, Olearnik H, Parker BC, Scott JE. Periprosthetic bone mineral density changes with femoral components of different design philosophy. In *Orthop*. 2001;25:89-92.
6. Glassman AH, Crowninshield RD, Schenck R, Herberts P. A low stiffness composite biologically fixed prostheses. *Clin Orthop*. 2001;393:128-36.
7. Tanzer M, Maloney WJ, Jasty M, Harris WH. The progression of femoral cortical osteolysis in association with total hip arthroplasty without cement. *J Bone Joint Surg Am*. 1992;74A:404-10.
8. Bugbee W, Culpepper W, Engh A, Engh CA. Long-term clinical consequences of stress-shielding after total hip arthroplasty without cement. *J Bone Joint Surg Am*. 1997;79A:1007-12.
9. Hellman EJ, Capello WN, Feinberg JR. Omnifit cementless total hip arthroplasty: A 10-years average follow up. *Clin Orthop*. 1999;364:164-74.
10. Engh CA Jr, Young AM, Engh CA Sr, Hopper RH Jr. Clinical consequences of stress shielding after porous-coated total hip arthroplasty. *Clin Orthop Relat Res*. 2003;417:157-63.
11. Sinha RK, Dungy DS, Yeon HB. Primary total hip arthroplasty with a proximally porous-coated femoral stem. *J Bone Joint Surg Am*. 2004;86A:1254-61.
12. Braun A, Papp J, Reiter A. The periprosthetic bone remodelling process signs of vital bone reaction. *Int Orthop*. 2003;27 Suppl 1:7-10.
13. Herrera A, Canales V, Anderson J, García-Araujo C, Murcia-Mazon A, Tonino AJ. Seven to ten years follow up of an anatomic hip prothesis. *Clin Orthop*. 2004;423:129-37.
14. Canales V, Panisello JJ, Herrera A, Peguero A, Martínez A, Herrero L, et al. Ten year follow-up of an anatomical hydroxyapatite-coated total hip prothesis. *Int Orthop*. 2006;30:84-90.
15. Tonino AJ, Therin M, Doyle C. Hydroxyapatite coated femoral stems: Histology and histomorphometry around five components retrieved at postmortem. *J Bone Joint Surg [Br]*. 1999;81B:148-54.
16. Nourissat C, Adrey J, Berteaux D, Gueret A, Goalard C, Hamon G. The ABG Standar hip prothesis: Five year results. En: *Epinette JA, Geesink RGT, editors. Hydroxyapatite coated hip and knee arthroplasty*. Paris: Edit Expansion Cientifique Francaise; 1995. p. 227-38.
17. Engh CA Jr, Mc Auley JP, Sychterz CJ, Sacco ME, Engh CA Sr. The accuracy and reproducibility of radiographic assessment of stress-shielding. *J Bone Joint Surg Am*. 2000;82A:1414-20.
18. Kröger H, Miettinen H, Arnala I, Koski E, Rushton N, Suomalainen O. Evaluation of periprosthetic bone using dual energy x-ray absorptiometry: precision of the method and effect of operation on bone mineral density. *J Bone Miner Res*. 1996;11:1526-30.
19. Rosenthal L, Bobyn JD, Tanzer M. Bone densitometry: influence of prosthetic design and hydroxyapatite coating on regional adaptative bone remodelling. *Int Orthop*. 1999;23:325-9.
20. Schmidt R, Nowak T, Mueller L, Pitto R. Osteodensitometry after total hip replacement with uncemented taper-design stem. *Int Orthop*. 2004;28:74-7.
21. Smart RC, Barbagallo S, Slater GL, Kuo RS, Butler SP, Drummond RP, et al. Measurement of periprosthetic bone density in hip arthroplasty using a dual energy X-ray absorptiometry. *J Arthroplasty*. 1996;11:445-52.
22. Panisello JJ, Herrero L, Canales V, Herrera A, Martínez A, Mateo J. Long-term remodelling in proximal femur around a hydroxyapatite-coated anatomic stem. Ten years densitometric follow-up. *J Arthroplasty*. 2008.
23. Oldani CR, Domínguez AA. Simulación del comportamiento mecánico de un implante de cadera. *Anales del 15.º Congreso Argentino de Bioingeniería*; Septiembre 2005. Ciudad de Paraná, Entre Ríos, Argentina. Soporte CD.
24. Torrenegra CA. Análisis estructural de endoprótesis para cadera, utilizando un modelo de elementos finitos. *Umbral Científico*. 2004;4:21-8.
25. Senalp AZ, Kayabasi O, Kurtaran H. Static, dynamic and fatigue behaviour of newly designed stem shapes for hip prothesis using finite element analysis. *Materials and Desing*. 2007;28:1577-83.
26. Kayabasi O, Erzincanli F. Finite element modelling and analysis of a new cemented hip prothesis. *Advances in Engineering Software*. 2006;37:477-83.
27. Domínguez-Hernández VM, Carbajal MF, Urriolagoitia G, Hernández LH, Rico G, Damián-Noriega Z, et al. Biomecánica de un fémur sometido a carga. Desarrollo de un modelo tridimensional por medio del método del elemento finito. *Rev Mex Ortop Traum*. 1999;13:633-8.
28. Zeman ME, Cerrolaza M, García JM, Doblaré M. Análisis comparativo F.E.M. 3D de la interacción entre el hueso femoral proximal y una prótesis de cadera utilizando un modelo de remodelación basado en mecánica del daño. Mérida (Venezuela): 5.º Congreso Iberoamericano de Ingeniería Mecánica; 2001 p. 69-74.
29. Domínguez-Hernández VM, Ramos VH, Feria CV, Urriolagoitia G, Hernández LH. Efecto del espesor de la capa de cemento en el componente femoral de una prótesis de Charnley. Análisis biomecánico mediante el método del elemento finito. *Rev Mex Ortop Traum*. 2000;14:443-8.
30. Kuiper JH, Huiskes R. The predictive value of stress shielding for quantification of adaptative bone resorption around hip replacement. *J Biomech Eng*. 1997;119:228-31.
31. Weinans H, Huiskes R, Grootenboer HJ. Effects of fit and bonding characteristics of femoral stems on adaptative bone remodelling. *J Biomech Eng*. 1994;116:393-400.
32. Kerner J, Huiskes R, van Lenthe GH, Weinans H, van Rietbergen B, Engh CA, et al. Correlation between pre-operative periprosthetic bone density and post-operative bone loss in THA can be explained by strain-adaptative remodelling. *J Biomech*. 1999;32:695-703.
33. Turner AWL, Gillies RM, Sekel R, Morris P, Bruce W, Walsh WR. Computational bone remodelling simulations and comparisons with DEXA results. *J Orthop Res*. 2005;23:705-12.
34. Karachalios T, Tsatsaronis CH, Efraimis G, Papadelis P, Lyritis G, Diakoumopoulos G. The long-term clinical relevance of calcar atrophy caused by stress shielding in total hip arthroplasty. *J Arthroplasty*. 2004;19:469-75.
35. Ohta H, Kobayashi S, Saito N, Nawata M, Horiuchi H, Takakura K. Sequential changes in periprosthetic bone mineral density following total hip arthroplasty: a 3-year follow-up. *J Bone Miner Metab*. 2003;21:229-33.
36. Nishii T, Sugano N, Masuhara K, Shibuya T, Ochi T, Tamura S. Longitudinal evaluation of time related bone remodelling after cementless total hip arthroplasty. *Clin Orthop Relat Res*. 1997;339:121-31.
37. Rahmy AI, Gosens T, Blake GM, Tonino A, Fogelman I. Periprosthetic bone remodelling of two types of uncemented fe-

- moral implant with proximal hydroxyapatite coating: a 3-year follow up study addressing the influence of prosthetic design and preoperative bone density on periprosthetic bone loss. *Osteoporos Int.* 2004;15:281-9.
38. Engh CA, Massin P, Suthers KE. Roentgenographic assessment of the biologic fixation of porous-surfaced femoral component. *Clin Orthop Relat Res.* 1990;257:107-28.
 39. Cohen B, Rushton N. Accuracy of DEXA measurement of bone mineral density after total hip arthroplasty. *J Bone Joint Surg Br.* 1995;77B:479-83.
 40. Mortimer ES, Rosenthal L, Paterson I, Bobyn JD. Effect of rotation on periprosthetic bone mineral measurements in a hip phantom. *Clin Orthop Relat Res.* 1996;324:269-74.
 41. I-DEAS; 2006. Disponible en: <http://www.ugs.com/>
 42. ABAQUS; 2006. Disponible en: <http://www.abaqus.com/>
 43. Arranz Merino S, Ros Felip A, Rincón Rincón E, Claramunt Alonso R. Caracterización mecánica del material óseo. *Tecnología y Desarrollo.* 2004;2:3-27.
 44. Evans FG. Mechanical properties of bone. En: Evans FG, editor. Illinois: Ed. Springfield; 1973.
 45. MatWeb (Material Property Data); 2006. Disponible en: <http://www.matweb.com/>
 46. Gutiérrez P, Doménech P, Roca J. Biomecánica de la cadera. En: Patología de la cadera en el adulto. Madrid: SECOT; 2004. p. 11-9.
 47. Rho JY, Hobatho MC, Ashman RB. Relations of mechanical properties to density and CT numbers in human bone. *Med Eng Phys.* 1995;17:347-55.
 48. Brodner W, Bitzan P, Lomoschitz F, Krepler P, Jankovsky R, Lehr S, et al. Changes in bone mineral density in the proximal femur after cementless total hip arthroplasty. A five-year longitudinal study. *J Bone Joint Surg Br.* 2004;86B:20-6.
 49. El Maraghy AW, Schemitsch EH, Waddell JP. Greater trochanter blood flow during total hip arthroplasty using a posterior approach. *Clin Orthop Relat Res.* 1999;363:151-7.
 50. Hupel TM, Schemitsch EH, Aksenov SA, Waddell JP. Blood flow changes to the proximal femur during total hip arthroplasty. *Can J Surg.* 2000;43:359-64.
 51. Korovessis P, Piperos G, Michael A, Baikousis A, Stamatakis M. Changes in bone mineral density around a stable uncemented total hip arthroplasty. *Int Orthop.* 1997;21:30-4.
 52. Kröger H, Venesmaa P, Jurvelin J, Miettinen H, Suomalainen O, Alhava E. Bone density at the proximal femur after total hip arthroplasty. *Clin Orthop.* 1998;352:66-74.
 53. Martini F, Leberher C, Mayer F, Leichtle U, Kremling E, Sell S. Precision of the measurements of periprosthetic bone mineral density around hips with a custom-made femoral stem. *J Bone Joint Surg Br.* 2000;82B:1065-71.
 54. Sychterz CJ, Claus AM, Engh CA. What we have learned about long-term cementless fixation from autopsy retrieval. *Clin Orthop Relat Res.* 2002;405:79-91.
 55. Kärrholm J, Anderberg CH, Snorrason F, Thanner J, Langgeland N, Malchau H, et al. Evaluation of a femoral stem with reduced stiffness. *J Bone Joint Surg Am.* 2002;84A:1651-8.
 56. Niinimäki T, Junila J, Jalovaara P. A proximal fixed anatomic femoral stem reduces stress shielding. *Int Orthop.* 2001;25:85-8.
 57. Zerahm B, Storgaard M, Johansen T, Olsen C, Lausten G, Kanstrup IL. Changes in bone mineral density adjacent to two biomechanically different types of cementless femoral stems in total hip arthroplasty. *Int Orthop.* 1998;22:225-9.
 58. Nagi ON, Kumar S, Aggarwal S. The uncemented isoelastic/isotitan total hip arthroplasty. A 10-15 years follow-up with bone mineral density evaluation. *Acta Orthop Belg.* 2006;72:55-64.
 59. Tonino A, Rahmy A. The hydroxyapatite ABG hip system. *J Arthroplasty.* 2000;15:274-82.
 60. Ahlborg H, Johnell O, Karlsson M. An age-related medullary expansion can have implications for the long-term fixation of hip prostheses. *Acta Orthop Scand.* 2004;75:154-9.
 61. Carrasco JL, Díaz M, Honorato J, Pérez R, Rapado A, Ruiz I. Densidad mineral ósea en cuello femoral. En: Proyecto Multicéntrico de Investigación en Osteoporosis. Estudio de la densidad ósea de la Población Española. Madrid: Pharma Consult editors; 1992.

Conflict of interests

The authors have stated they have no conflict of interests.